ciation of SODD with the uncomplexed TNF-R1 then reestablishes the normal silent state for TNF-R1. This tight control of the duration of TNF signaling at the receptor level is somewhat analogous to the temporal regulation of NF-κB activity by the NF-κB inhibitor IκB that occurs downstream in the TNF signaling cascade. In addition to its role as a silencer of TNF-R1 signaling, we have considered the possibility that SODD may also participate in transducing TNF signals once it is released from the activated receptor complex. However, at this time, we have no evidence for such a signaling role.

It is likely that SODD also functions as an inhibitor of constitutive DR3 signaling because (i) SODD interacts with DR3 and TNF-R1 equally well in yeast two-hybrid and mammalian coprecipitation assays; (ii) DR3, like TNF-R1, signals independently of ligand when overexpressed (*16*); (iii) the death domains of DR3 and TNF-R1 are highly related, sharing 45% sequence identity; and (iv) TNF-R1 and DR3 both use TRADD, TRAF2, RIP, and FADD for signal transduction (*16*). Finally, on the basis of these results, we predict that SODD-related proteins will be found that interact with and play a similar role in preventing spontaneous signaling by Fas, DR4, and DR5. In fact, a candidate protein having 61% identity to the COOH-terminal 71 amino acids of SODD is predicted to be encoded by expressed sequence tag cDNA clones (*17*) found in the National Center for Biotechnology Information DNA database.

References and Notes

1. L. A. Tartaglia and D. V. Goeddel, *Immunol. Today* **13**, 151 (1992); P. Vandenabeele, W. Declercq, R. Beyaert, W. Fiers, *Trends Cell Biol.* **5**, 392 (1995).
2. L. A. Tartaglia, T. M. Ayres, G. H. W. Wong, D. V. Goeddel, *Cell* **74**, 845 (1993).
3. H. Hsu, J. Xiong, D. V. Goeddel, *ibid.* **81**, 495 (1995).
4. D. W. Banner *et al.*, *ibid.* **73**, 431 (1993).
5. H. Hsu, H.-B. Shu, M.-P. Pan, D. V. Goeddel, *ibid.* **84**, 299 (1996).
6. W.-C. Yeh *et al.*, *Science* **279**, 1954 (1998).
7. Z. Liu, H. Hsu, D. V. Goeddel, M. Karin, *Cell* **87**, 565 (1996); W.-C. Yeh *et al.*, *Immunity* **7**, 715 (1997).
8. H. Hsu, J. Huang, H.-B. Shu, V. Baichwal, D. V. Goeddel, *Immunity* **4**, 387 (1996); M. A. Kelliher *et al.*, *ibid.* **8**, 297 (1998).
9. A. Ashkenazi and V. M. Dixit, *Science* **281**, 1305 (1998).
10. H. Y. Song, J. D. Dunbar, D. B. Donner, *J. Biol. Chem.* **269**, 22492 (1994); M. P. Bolden *et al.*, *ibid.* **270**, 387 (1995).
11. The plasmid Gal4BD-DR3, which encodes the GAL4 DNA-binding domain fused to the intracellular domain (amino acids 227 to 418) of DR3, was used as bait in a yeast two-hybrid screen of a HeLa cell cDNA library (Clontech). The isolated positive clones were analyzed as described (*3*). Full-length SODD cDNA was obtained by screening a λZAP human Jurkat T cell cDNA library by standard methods (*3*).
12. Y. Jiang, W. Liu, D. V. Goeddel, unpublished data.
13. For protein-protein interaction assays, subconfluent 10-cm dish cultures of 293 cells were transfected by the calcium phosphate method (*3*). To determine SODD interaction with DDRs, we used expression vectors encoding Flag-SODD and GST-DDRs or GST. Twenty-four hours after transfection, cells were washed in phosphate-buffered saline and lysed in E1A lysis buffer (*3*). Lysates were precipitated with glutathione agarose beads (Pharmacia Biotechnology), and the beads were washed three times with E1A buffer and twice with E1A buffer containing 1 M NaCl. The precipitates were fractionated on SDS–polyacrylamide gel electrophoresis (SDS-PAGE) and transferred to a nitrocellulose membrane. The coprecipitated SODD was detected by immunoblot analysis with polyclonal antibodies to the Flag epitope (Santa Cruz Biotechnology). To determine SODD binding to various TNF-R1 mutants (*2*, *3*), we incubated cell lysates for 2 to 4 hours at 4°C with monoclonal antibody 985 to TNFR1 (*5*) or control mouse immunoglobulin G (IgG) monoclonal antibody (Sigma) and 25 μl of 1:1 slurry of protein G–Sepharose (Pharmacia). Beads were washed twice with 1 ml of E1A buffer, twice with 1 ml of high salt E1A buffer, and twice again with E1A buffer before immunoblot analysis was performed.
14. H.-B. Shu, M. Takeuchi, D. V. Goeddel, *Proc. Natl. Acad. Sci. U.S.A.* **93**, 13973 (1996).
15. M. Tanaka and D. V. Goeddel, unpublished data.
16. A. M. Chinnaiyan *et al.*, *Science* **274**, 990 (1996); J. Kitson *et al.*, *Nature* **384**, 372 (1996); S. Marsters *et al.*, *Curr. Biol.* **6**, 1669 (1996).
17. GenBank accession numbers AA319013, AA362082, H10621, and T33545.
18. Rabbit polyclonal antisera were generated against a SODD peptide (amino acids 292 to 313) and against purified His-tagged SODD produced in *Escherichia coli*. The upper band of the protein doublet in Fig. 1C is presumably phosphorylated SODD. This band predominates in cell lines that express low levels of SODD, whereas both bands are apparent in cell lines that express higher levels (*12*).
19. J. D. Woronicz, X. Gao, Z. Cao, M. Rothe, D. V. Goeddel, *Science* **278**, 866 (1997).

20. We thank L. Huang for synthesizing the SODD peptide for antibody generation, V. Dixit for providing the DR3 cDNA, A. Ashkenazi for providing DR4 and DR5 cDNAs, D. Baltimore for supplying the parental mammalian cell expression vector for GST, pEBG, and L. Medin for help with the figures.

9 October 1998; accepted 21 December 1998

Silencing of Genes Flanking the P1 Plasmid Centromere

Oleg Rodionov, Małgorzata Łobocka,* Michael Yarmolinsky†

Partition modules stabilize bacterial plasmids and chromosomes by actively promoting their segregation into daughter cells. The partition module of plasmid P1 is typical and consists of a centromere site, *parS*, and genes that encode proteins ParA and ParB. We show that ParB can silence genes flanking *parS* (to which ParB binds), apparently by polymerizing along the DNA from a nucleation site at *parS*. Wild-type ParB contacts an extensive region of P1 DNA; silencing-defective ParB proteins, which were found to be partition-defective, are less able to spread. Hence, the silenced structure appears to function in partitioning.

In eukaryotes, transcriptional silencing of DNA regions, which range in size from short segments to entire chromosomes, is an essential feature of development (*1*). In fission yeast and in *Drosophila*, extensive regions of silencing that spread from centromeric sites appear to be necessary for full centromere functioning (*2*). We consider the possibility that silencing may have a role in the prokaryotic equivalent of mitosis—the process of partitioning plasmids and chromosomes (ensuring their orderly segregation to daughter cells). Knowledge of partitioning has been mainly derived from studies of plasmid-encoded partitioning genes and their chromosomal homologs, which have been recognized to be present in diverse bacteria (*3–5*). Although the few reports of silencing in bacteria are generally of silencing over short regions, studies have shown that genes several kilobases distant from the centromere of the bacterial plasmid F can be silenced by high levels of the F partition protein, SopB (*6, 7*). Here, we characterize silencing by comparable elements of the P1 plasmid, provide evidence concerning its mechanism, and assess its relevance for partitioning.

P1 partitioning requires two P1 proteins (ParA and ParB) and a DNA site (*parS*) (*8*). ParB binds to *parS* (*9, 10*); ParA is an adenosine triphosphatase (*11*). These factors, together with unknown host components, ensure plasmid stability. We previously observed that, dependent on the location of *parS*, ParB can either destabilize a *parS*-bearing plasmid (*12*) or prevent such a plasmid from conferring antibiotic resistance (*13*), perhaps by gene silencing in each case. To further study silencing, we inserted *parS* and reporter genes *lacZ* and *cat* at the λ attachment site (*att*λ) of *Escherichia coli*, close to the biotin biosynthesis genes (*bioA*, *B*, *F*, *C*, and *D*) (Fig. 1A). We made constructs with *parS* in opposite orientations (I and II) and a construct without *parS* (0). ParB was supplied from an inducible plasmid source.

Expression of the *cat*, *lacZ*, and *bio* genes was markedly decreased by the presence of wild-type ParB, in contrast to their expression in controls that lacked *parS* or in which

Laboratory of Biochemistry, National Cancer Institute, 37 Convent Drive, Bethesda, MD 20892–4255, USA.

*Present address: Department of Microbial Biochemistry, Institute of Biochemistry and Biophysics, Polish Academy of Sciences, ul. Pawińskiego 5A, 02-106, Warsaw, Poland.

†To whom correspondence should be addressed. E-mail: myarmo@helix.nih.gov

ParB was binding-defective. With increasing ParB, the expression of *lacZ* diminished rapidly (Fig. 1B). ParB was required in larger amounts to diminish expression of the more distant *cat*. At no tested concentration did ParB diminish expression of *phoA*, which is a gene much farther from *parS* (Fig. 1B). The amount of ParB generated by a wild-type P1 plasmid was sufficient to reduce the expression of *lacZ* in construct I by ~50%, which suggests that ParB-mediated gene silencing might have a physiological function. Silencing extended in both directions for several kilobases, but the reduction in gene expression was greatest to the side of *parS* that, in P1, would face away from the partition genes, which lie upstream (Fig. 1C). A decrease in the efficiency of ParB-mediated silencing was expected to occur in the absence of the architectural protein IHF (integration host factor), because IHF strongly promotes the binding of ParB to *parS* in vitro and, to a lesser extent, assists in P1 partitioning (*9, 14*). Our expectation was confirmed, although the decrease in silencing due to an *ihfA* mutation was largely to one side of *parS* (Fig. 1C).

Might *parS* act as a nucleation site for ParB polymerization along the DNA? Although the SopB protein of plasmid F, by itself, was found to be incapable of forming nucleoprotein filaments with linear DNA in vitro (*7*), it seemed likely that SopB and its homolog (ParB), in view of their abundance, could be primary protein components of such filaments. A demonstration that ParB is specifically associated with the silenced region of the DNA was achieved by formaldehyde-mediated DNA-protein cross-linking followed by immunoprecipitation and polymerase chain reaction (PCR) analysis of the DNA that was released by heating the precipitate (Fig. 2A). Mutant ParB (Δ263-333) that was unable to bind to *parS* did not associate with DNA in any of the tested regions.

Cross-linking experiments were also performed with nine ParB mutants that had been isolated as being unable to destabilize the ParB-sensitive plasmid pMLO6 and that had been selected as being capable of binding *parS* in vitro (*12*). These mutants were totally silencing-defective (*15*), and in addition, each of them had been previously found to be partitioning-defective. Upon in vivo treatment with formaldehyde, each of the mutant proteins showed the expected, if somewhat attenuated, cross-linking to *parS* (Fig. 2B). No mutant exhibited DNA binding outside *parS*, with the exception of $Ile^{105} \rightarrow Thr^{105}$ (I105T). These results suggest that ParB polymerization beyond *parS* is necessary, although not sufficient, for the ParB-mediated silencing. Because the mutants are partitioning-defective, ParB polymerization could also be important in the partitioning process.

In principle, the growth of a filament nucleated at *parS* and spreading outward might be blocked by a protein that is tightly bound to a DNA locus in its path. We investigated whether a "roadblock" interposed between *parS* and a reporter gene would alleviate silencing of the reporter. A set of tandem sites to which the P1-encoded replication initiator protein (RepA) can bind tightly was tested for this capacity. How growth of the nucleoprotein filament might be stopped by RepA protein, acting as a repressor, is shown schematically (Fig. 3A). Strains that are similar to those in Fig. 1 were used; however, the promoter-operator region of the P1 *repA* gene (controlling *lacZ*) included all five RepA binding sites rather than just one. RepA was supplied constitutively. The bound repressor completely alleviated silencing of the *cat* gene, which is distal to the roadblock and is 4 kilobases (kb) away, but did not prevent ParB from silencing the *bio* locus, as judged by continued auxotrophy for biotin (Fig. 3A). A specific association of ParB with the silenced regions flanking *parS* (but only a minimal association with DNA distal to a roadblock, including DNA within *lacZ*) was shown by the formaldehyde cross-linking technique (Fig. 3B). Controls in which an antibody to RepA was used showed that RepA could be cross-linked to DNA that included its operator sites and to no DNA of other regions tested. The largely unilateral alleviation of silencing in an *ihfA* mutant (Fig. 1C) might be interpreted as a consequence of a facilitation of ParB binding to *parS* while blocking propagation of silencing from the side of *parS* that contains most of the ParB-binding boxes (Fig. 1A) and that is essential and sufficient for ParB binding and partitioning (*16*).

If an association of ParB with DNA outside of *parS* is to have a role in partitioning, then such an association should be demonstrable in formaldehyde-treated cells carrying a P1 plasmid. Our study showed that ParB could be cross-linked to P1 DNA over at least 11 kb, of which 8 kb are downstream of the *par* operon (Fig. 4). Possibly, most of the 7000 ParB dimers reported to be present in a bacterium carrying P1 (*17*) are bound with DNA. The notion that a genetically silenced nucleoprotein filament extending beyond the limits of a plasmid centromere might function in partitioning is supported by two additional considerations. First, the capacity for gene silencing is common to the centromere-binding proteins of P1 and F plasmids (*6*) and their nonhomologous analog (ParR) of plasmid R1 (*18*). Second, the capacities of ParB for gene silencing and for partitioning are altered by the same mutations. Thus, prokaryotic centromere function may depend on a capacity to seed a nucleoprotein filament.

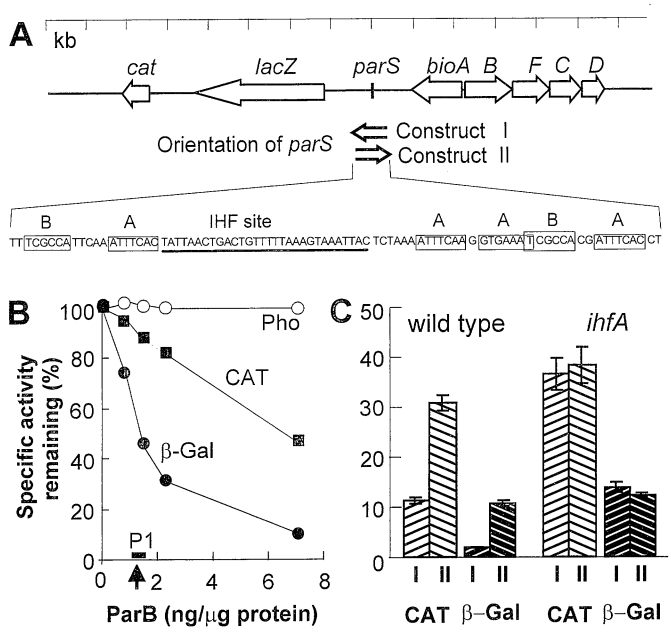

Fig. 1. (**A**) Map of region flanking *parS* in tester strains (*28*). Within the *parS* sequence (shown oriented as in construct II), heptameric "A" and hexameric "B" sites to which ParB binds (*10*) are boxed; the binding site of IHF is underlined. (**B**) Relation between ParB concentration and expression of *lacZ*, *cat*, and *phoA* in construct I. Specific activities of chloramphenicol acetyltransferase (CAT), β-galactosidase (β-Gal), and constitutive alkaline phosphatase (Pho) were determined by spectrophotometric methods (*27*) in cultures of strains carrying an inducible source of ParB, pOAR32, or the corresponding vector (*29*). Results of typical experiments are shown; remaining specific activity is relative to specific activity in "no ParB" (vector) controls. The ParB concentration in construct 0 (no *parS*) carrying a P1 marked with a kanamycin-resistance determinant (*30*) is included for comparison (represented as the P1 bar). ParB that was supplied at concentrations sufficient to reduce *lacZ* expression by 90% in construct I caused no reduction in construct 0 (499 ± 5 compared to 517 ± 18 Miller units in "no ParB" controls). (**C**) Effect of an *ihfA* mutation on the silencing of *lacZ* and *cat* in constructs I and II. ParB was supplied to constructs I and II (or to their Δ*ihfA*::Tn*10* derivatives) from pBR327P*trp*-*parB* (pMLO102) or from the corresponding plasmid bearing the Δ263-333 variant (*12*). Bacteria were grown in the presence of 3-β-indoleacrylic acid (100 μg/ml) as inducer (*31*) for about six generations. Results are the average of three determinations.

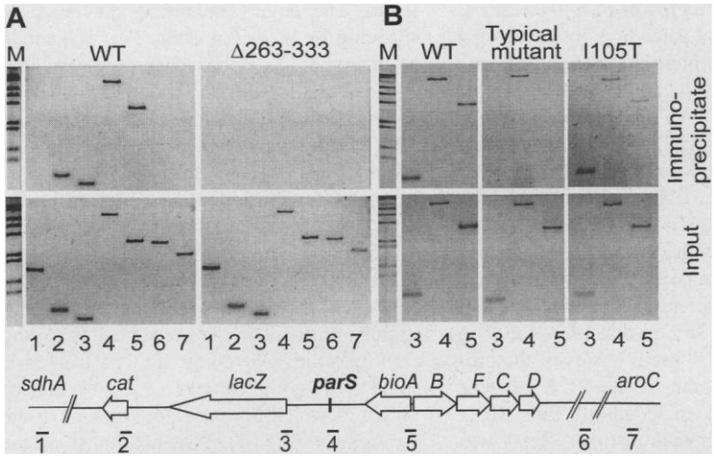

Fig. 2 (left). Identification of immunoprecipitated DNA that was cross-linked with formaldehyde in vivo to ParB (construct I) (**A**) Association of DNA with wild-type (WT) ParB. Cells of the tester strain were fixed with formaldehyde, lysed, and sonicated to reduce the average size of the DNA to 0.5 to 1 kb; the DNA that was associated with ParB was immunoprecipitated as described (*5*), except that the lysis buffer contained ribonuclease. Cells containing binding-defective ParBΔ263-333 served as a negative control. DNA fragments released from immunoprecipitates and from whole cell extracts (input) were identified by PCR amplification with primer pairs from the indicated (numbered) locations along the DNA (*32*). The templates for primer pairs "1," "6," and "7" were located 50 kb to the left of *parS* in the *sdhA* gene of *E. coli*, 50 kb to the right of *parS* in an open reading frame of unknown function, and at the chromosomal antipode in the *E. coli aroC* gene, respectively. PCR products were electrophoresed through a 3.5% agarose gel, stained with ethidium bromide, and photographed, and these images were processed. Lane numbers correspond to those of the relevant primer pairs; M, marker lanes. (**B**) Association of DNA with ParB of silencing-defective ParB mutants. Experimental conditions were as in (A). Results obtained with mutants Q88L, I94T, T145P, Q148R, V201Q, E204G, E204K, and D250V (*33*) were indistinguishable and are represented in the panel labeled "Typical mutant."

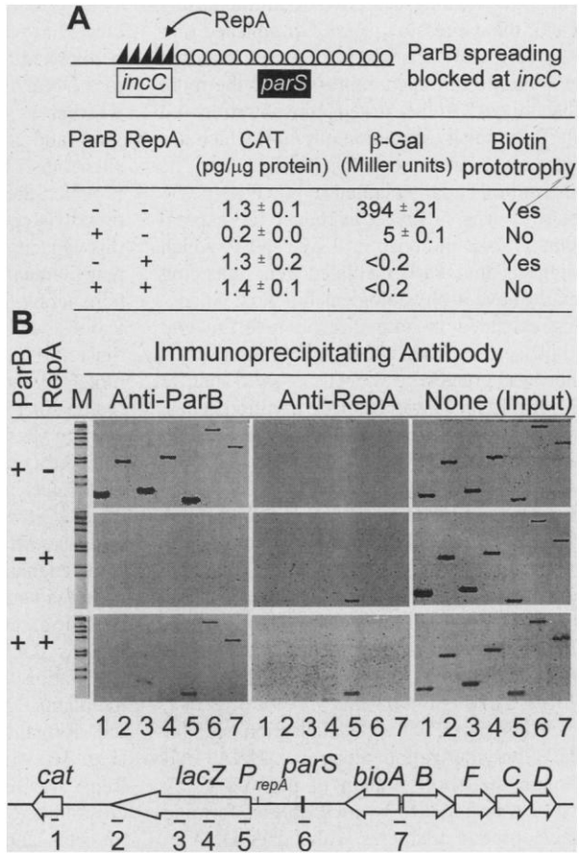

Fig. 3 (right). (**A**) A protein-DNA complex acting as a roadblock to the spread of silencing. In the schematic diagram, circles represent ParB, and triangles represent repressor (RepA) that is tightly bound to sites at the operator (incC) of the P_{repA} (*34*) from which *lacZ* is transcribed in the tester strain. Bacterial strains were identical to constructs I and II (Fig. 1) except that P_{repA} with a single ParB binding site was replaced by the entire P1 *incC* region encompassing P_{repA} and five tandem sites to which RepA binds tightly. ParB was supplied from pOAR32 (*27*) containing parB under P_{tac} control, and RepA was supplied from pALA162 (*35*) containing *repA* under *bla*-P2 control. Vectors without functional *parB* and *repA* were used to make the strains being compared otherwise isogenic. The presence of kanamycin (25 μg/ml) and ampicillin (100 μg/ml) ensured plasmid retention. Growth with IPTG (1 mM) for about seven generations served to induce ParB synthesis and dilute protein that was accumulated before silencing. Two or three independent transformants of each kind were assayed for the indicated gene functions in triplicate. CAT protein relative to total protein was measured by an enzyme-linked immunosorbent assay (Boehringer-Mannheim). Beta-galactosidase was measured as previously described (Fig. 1B). Dependence of colonial growth in minimal-glucose medium on added biotin (seen only when ParB was supplied to construct II) was scored as an absence of prototrophy ("No"). (**B**) The protein-DNA complex acting as a roadblock to the spread of ParB along the DNA. Bacterial constructs were as in (A), except that only strains with *parS* in orientation I were used. DNA associated with ParB or with RepA was identified by PCR (as in Fig. 2) after immunoprecipitation with the indicated antibodies. (M, marker lanes in gels.)

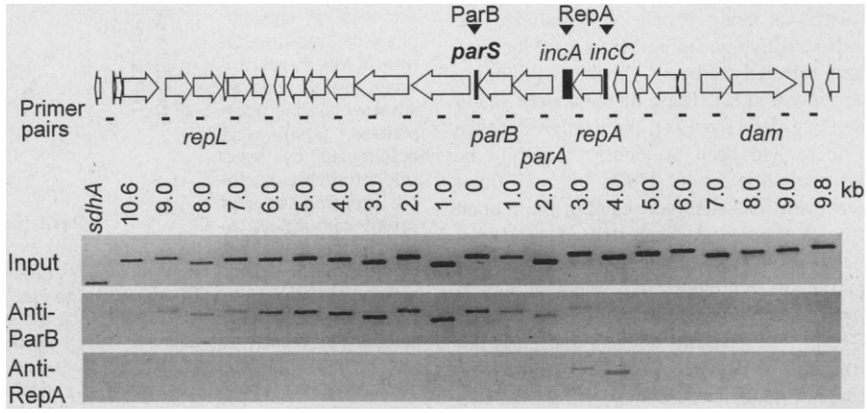

Fig. 4. In vivo association of ParB and RepA with P1 DNA. Electrophoresed PCR products that identify the DNA that was specifically cross-linked in vivo to ParB and RepA of a P1 plasmid are shown. Cells of the P1-carrying strain (Fig. 1B) were treated as described (Fig. 2), with antibodies to ParB and antibodies to RepA for immunoprecipitations. The locations of primer pairs along the DNA of P1 in the regions flanking *parS* are shown with respect to a physical map of known and putative genes (arrows) and the binding sites (solid rectangles) of plasmid proteins ParB and RepA (*36*). The leftmost primer pair was "1" of Fig. 2A. The unlabeled genes between *repL* and *dam* are of unknown function. Genes between *parS* and *repL* are under the control of a late promoter. The regions that are cross-linked to RepA correspond to two sets of RepA binding sites: *incC*, within the P1 plasmid origin of replication, and *incA*, a separate replication-control locus. Samples taken for PCR amplification of input DNA, of DNA immunoprecipitated with antibodies to ParB, and of DNA immunoprecipitated with antibodies to RepA were diluted 1:1000, 1:250, and 1:25, respectively.

The filament (shown in Fig. 3A as a linear structure for simplicity) is more likely to be compacted in a solenoid in which the DNA wraps through multiple turns about a protein core, as was suggested by the observed changes in linking numbers upon formation of a SopB-DNA complex (*19*).

Prokaryotic centromeres are characterized by the presence of arrays of sites to which one of the partition proteins bind. There are 6 sites in P1 (Fig. 1A), 12 in F, 10 in R1, and 12 in pTAR (*20*). Whereas these plasmid-borne binding sites are tightly clustered, the several chromosomal binding sites for the *Bacillus subtilis* partition (and sporulation) protein Spo0J are distributed over a region spanning many kilobases (*3*). The centromere may serve as a handle that is used to tether or orient a large structure, with its several binding sites facilitating a steady grip or the formation of an intermediate that is appropriately paired for partitioning. Evidence for paired intermediates in the partitioning of plasmid R1 and involving its cognate ParB analog has recently been obtained (*21*). Like the proteins of heterochromatin that spread from centromeres or telomeres of eukaryotic chromosomes, the ParB that spreads from the P1 plasmid centromere can silence genes. In each case, this capacity for gene silencing may be incidental to a primary structural role that is associated with DNA segregation or movement.

References and Notes

1. E. A. Russo, R. A. Martienssen, A. D. Riggs, Eds., *Epigenetic Mechanisms in Gene Regulation* (Cold Spring Harbor Laboratory Press, Plainview, NY, 1996).
2. R. C. Allshire, E. R. Nimmo, K. Ekwall, J. P. Javerzat, G. Cranston, *Genes Dev.* **9**, 218 (1995); G. H. Karpen, *Curr. Opin. Genet. Dev.* **4**, 281 (1994).
3. D. C.-H. Lin, P. A. Levin, A. D. Grossman, *Proc. Natl. Acad. Sci. U.S.A.* **94**, 4721 (1997).
4. D. A. Mohl and J. W. Grober, *Cell* **88**, 675 (1998); C. D. Webb *et al.*, *ibid.*, p. 667.
5. D. C.-H. Lin and A. D. Grossman, *ibid.* **92**, 675 (1998).
6. A. S. Lynch and J. C. Wang, *Proc. Natl. Acad. Sci. U.S.A.* **92**, 1896 (1995); S.-K. Kim and J. C. Wang, *ibid.* **95**, 1523 (1998).
7. R. Hanai *et al.*, *J. Biol. Chem.* **271**, 17469 (1996).
8. A. L. Abeles, S. A. Friedman, S. J. Austin, *J. Mol. Biol.* **185**, 261 (1985); published errata, *ibid.* **189**, 387 (1986).
9. B. E. Funnell, *J. Biol. Chem.* **266**, 14328 (1991).
10. _____ and L. Gagnier, *ibid.* **268**, 3616 (1993); F. Hayes and S. J. Austin, *Proc. Natl. Acad. Sci. U.S.A.* **90**, 9228 (1993).
11. M. A. Davis, K. A. Martin, S. J. Austin, *Mol. Microbiol.* **6**, 1141 (1992).
12. M. Łobocka and M. Yarmolinsky, *J. Mol. Biol.* **259**, 366 (1996).
13. The *parS*-bearing plasmid pMLO6 (*12*) could not be maintained in the presence of a source of ParB. By moving *parS* ~180° from its position in pMLO6, a plasmid was created that, in the presence of ParB, no longer conferred spectinomycin resistance but had become only moderately unstable. The altered distance of *parS* from the DNA loci that are involved in replication and in the expression of antibiotic resistance can account for the difference in phenotypes.
14. B. E. Funnell, *Proc. Natl. Acad. Sci. U.S.A.* **85**, 6657 (1988).
15. O. Rodionov and M. Yarmolinsky, data not shown.
16. K. A. Martin, M. A. Davis, S. J. Austin, *J. Bacteriol.* **173**, 3630 (1991); M. Łobocka and M. Yarmolinsky, unpublished material.
17. B. E. Funnell and L. Gagnier, *Biochimie* **76**, 924 (1994).
18. K. Gerdes, unpublished material.
19. D. P. Biek and J. Shi, *Proc. Natl. Acad. Sci. U.S.A.* **91**, 8027 (1994); A. S. Lynch and J. C. Wang, *J. Mol. Biol.* **236**, 679 (1994).
20. M. Helsberg and R. Eichenlaub, *J. Bacteriol.* **165**, 1043 (1986); M. Dam and K. Gerdes, *J. Mol. Biol.* **236**, 1289 (1994); D. R. Gallie and C. L. Kado, *ibid.* **193**, 465 (1987).
21. R. B. Jensen, R. Lurz, K. Gerdes, *Proc. Natl. Acad. Sci. U.S.A.* **95**, 8550 (1998).
22. K. F. Wertman, A. R. Wyman, D. Botstein, *Gene* **49**, 253 (1986).
23. L. Diederich, L. J. Rasmussen, W. Messer, *Plasmid* **28**, 14 (1992).
24. P. P. Papp, G. Mukhopadhyay, D. K. Chattoraj, *J. Biol. Chem.* **269**, 23563 (1994).
25. T. Som and J.-I. Tomizawa, *Mol. Gen. Genet.* **187**, 375 (1982).
26. V. M. Morales, A. Baeckman, M. Bagdasarian, *Gene* **97**, 39 (1991).
27. J. H. Miller, *Experiments in Molecular Genetics* (Cold Spring Harbor Laboratory Press, Plainview, NY, 1972); W. V. Shaw, in *Antibiotics*, vol. 43 of *Methods in Enzymology*, J. H. Hash, Ed. (Academic Press, New York, 1975), pp. 737–755; E. Brickman and J. Beckwith, *J. Mol. Biol.* **96**, 307 (1975).
28. Constructs 0, I, and II were derived from a *recA56* MC1061 (*22*) by the integration of *parS*, *lacZ*, and *cat* into *attλ* (*23*). The *lacZ* gene under control of the P1 *repA* promoter (P_{repA}), accompanied upstream by four *rrnB* T1 transcription terminators, was from pPP112 (*24*). The source of *parS* was a 298–base pair Eco RI fragment from pBEF143 (*9*). The *cat* gene was from pST52 (*25*). A mutant version of construct I that is constitutive for *phoA* expression was used for the alkaline phosphatase assay. Gene orientations and the absence of duplicate insertions were determined by restriction mapping.
29. To construct pOAR32, we cloned the *parB* gene under tac promoter (P_{tac}) control in a derivative of pMMB67EH (*26*) in which the kanamycin-resistance gene of transposon (Tn) *903* had been inserted so as to disrupt the *bla* gene of the vector. For assays, cultures were grown in LB broth (*27*) with kanamycin (25 mg/ml) and, subsequently, for about six generations, with isopropyl-β-D-thiogalactopyranoside (IPTG) at several concentrations before the measurement of enzyme specific activities. The ParB concentration in sonicated cell extracts was estimated by the ECL protein immunoblotting analysis system (Amersham) with highly purified ParB as standard.
30. T. Takano and S. Ikeda, *Virology* **70**, 198 (1976).
31. B. P. Nichols and C. Yanofsky, in *Recombinant DNA, Part C*, vol. 101 of *Methods in Enzymology*, R. Wu, L. Grossman, K. Moldave, Eds. (Academic Press, New York, 1983), pp. 155–164.
32. Template DNAs were purified with a high pure PCR template preparation kit (Boehringer Mannheim) and, unless otherwise indicated, used at a dilution of 1:850. PCR reactions were performed with 100 pmoles of each primer and 0.25 units of Taq polymerase in B buffer (Promega) in 50-μl volumes as follows: An initial denaturation at 95°C for 2 min was followed by 25 cycles with denaturation for 30 s at 95°C, annealing for 30 s at 61°C (at 54°C with primers directed against P1 DNA), polymerization for 1 min at 72°C, and a final 2-min extension at 72°C.
33. Single-letter abbreviations for the amino acid residues are as follows: D, Asp; E, Glu; G, Gly; I, Ile; K, Lys; L, Leu; P, Pro; Q, Gln; R, Arg; T, Thr; and V. Val.
34. A. L. Abeles, K. M. Snyder, D. K. Chattoraj, *J. Mol. Biol.* **173**, 307 (1984).
35. D. K. Chattoraj, K. Cordes, A. L. Abeles, *Proc. Natl. Acad. Sci. U.S.A.* **81**, 6456 (1984).
36. M. Łobocka, M. Rusin, A. Samojedny, unpublished material.

37. We thank D. K. Chattoraj for valuable discussions, bacterial strains, plasmids, and antibody to RepA, and, with R. A. Weisberg, for critical readings of early versions of the manuscript; K. Gerdes for permission to cite unpublished material; B. E. Funnell for a sample of highly purified ParB; and D. C.-H. Lin for the cross-linking immunoprecipation protocol that he developed in the A. D. Grossman laboratory. O.R. and M.L. were supported by Fogarty postdoctoral fellowships.

17 August 1998; accepted 22 December 1998

The Role of Locus Coeruleus in the Regulation of Cognitive Performance

Marius Usher, Jonathan D. Cohen, David Servan-Schreiber, Janusz Rajkowski, Gary Aston-Jones*

Noradrenergic locus coeruleus (LC) neurons were recorded in monkeys performing a visual discrimination task, and a computational model was developed addressing the role of the LC brain system in cognitive performance. Changes in spontaneous and stimulus-induced patterns of LC activity correlated closely with fluctuations in behavioral performance. The model explains these fluctuations in terms of changes in electrotonic coupling among LC neurons and predicts improved performance during epochs of high coupling and synchronized LC firing. Cross correlations of simultaneously recorded LC neurons confirmed this prediction, indicating that electrotonic coupling in LC may play an important role in attentional modulation and the regulation of goal-directed versus exploratory behaviors.

Neuromodulators, such as norepinephrine (NE) and dopamine, have long been thought to play a role in regulating nonspecific aspects of behavior, such as motivation and arousal. However, recent evidence indicates that these systems may play a more specific role in task-related cognitive processes. Brainstem dopaminergic neurons respond selectively to stimuli that predict reward (*1*). Stimulus-specific activity has also been observed in LC neurons. Recent studies found that LC neurons in monkeys performing a visual discrim-